

- ◆ Recepción/ 27 junio 2019
- ◆ Aceptación/ 25 agosto 2019

Significant Enhancement in Hydrogen Sensing using Boron nitride Wurtzoid Structures

Mejora significativa en la detección de hidrógeno usando estructuras de Wurtzoid de nitruro de boro

**Bilal K. Al-Rawi^{1*} ,
Safaa M. Al-Janabi²**

¹University of Anbar, College of Education for Pure Science, Anbar, Iraq.

²Knowledge University, College of Engineering, Petroleum Engineering Department.

E-mail: bilal_al_rawi@yahoo.com

ABSTRACT/ The structural and vibration properties of Boron Nitride (BN) have been identified for each passivated hydrogen and bare in nanostructure. The B sites in BN wurtzoid are founded to be either oxidized or entirely related through nitrogen or hydrogen molecules and the forces between the molecules are van der Waals' forces. However, the N sites structure has been used to detect the hydrogen molecules. Boron nitride wurtzite nanocrystals are investigated to determine the wurtzoid molecular building blocks. The bulk gap of experimental results is generally constrained between the bare and Hydrogen (H) passivated wurtzoids shown in results. The parameters of structural properties, including bonds lengths and angles are in a great match with the practical results founded previously. Modeled BN wurtzite nanostructure showed appropriate choice for the hydrogen sensing, highly close to the more stable states, in a good similarity with the practical results.

Keywords: BN; DFT; Nanocrystals Properties, wurtzoid, wurtzite, building blocks.

RESUMEN/ Las propiedades estructurales y de vibración del nitruro de boro (BN) se han identificado para cada hidrógeno pasivado y desnudo en nanoestructura. Los sitios B en el wurtzoide BN se encuentran oxidados o completamente relacionados a través de moléculas de nitrógeno o hidrógeno y las fuerzas entre las moléculas son las fuerzas de van der Waals. Sin embargo, la estructura de los sitios N se ha utilizado para detectar las moléculas de hidrógeno. Los nanocristales de wurtzita de nitruro de boro se investigan para determinar los bloques de construcción moleculares de wurtzoide. La brecha general de los resultados experimentales generalmente está limitada entre los wurtzoides desnudos y pasivados con hidrógeno (H) que se muestran en los resultados. Los parámetros de las propiedades estructurales, incluidas las longitudes de los enlaces y los ángulos, coinciden en gran medida con los resultados prácticos fundados anteriormente. La nanoestructura modelada de wurtzita BN mostró la elección apropiada para la detección de hidrógeno, muy cerca de los estados más estables, en buena similitud con los resultados prácticos.

Palabras llave: BN; DFT Propiedades de nanocristales, wurtzoide, wurtzita, bloques de construcción.

Introduction

Boron nitride is a chemical compound of boron and nitrogen, which has the chemical formula BN. The compound belongs with a group of nitrides as solid, colorless semiconductor. There are four essential forms (structures) of boron nitride, the first structure is the amorphous form (α -BN), which is non-crystalline, while all other boron nitride forms are crystalline. The other three forms are (α -

BN, β -BN and w-BN) respectively, α -BN which has a hexagonal structure (analogous to graphite) called hBN. β -BN which has a cubic structure (analogous to diamond) cBN. Finally wurtzite form (analogous to lonsdaleite) referred as w-BN. The different angles between neighboring tetrahedral and the rings between layers are in w-BN configuration. The form of wurtzite is considered to be very strong and it was estimated by simulation

methode having a potential strength 18% stronger than diamond. These nitrides span many applications, including LEDs, optoelectronics and solar cells [1, 2]. Several nanocrystals applications revealed more relative potential properties that are unbeknown and have to be correlated theoretically and experimentally. Figure (1) gives a comparison between the crystalline boron nitride forms.

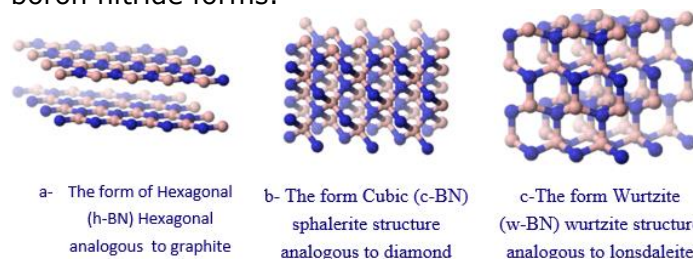


Figure (1) The BN crystalline structure comparison.

BN nanotubes (BNNTs) are a polymorph of boron nitride Similar to the carbon nanotubes, which are cylinders with sub-micrometer diameters and micrometer lengths, except that nitrogen and boron atoms alternatively substitute atoms of carbon. However, BN nanotubes properties are very different, while, the nanotubes of carbon may be semiconducting or metallic depending on the rolling direction and radius, a BN nanotube is an electrical insulator with a bandgap of ~ 5.5 eV, mostly tube chirality independent and morphology [3]. Moreover, a layered BN structure is much greater stable thermally and chemically than a graphitic structure of carbon [4, 5]. Diamondoids that diamond and zincblende materials molecular building blocks [4]. The study of diamondoids is strictly regarding BN [5]; the lattice constant must be nearly the same. However, BN diamondoids had not been inspected. Mechanical, electronic and optical properties for many materials are changed when transforms into their nanoscales [6] also the size changed.

The research is based novelty on the possible main enhancement. The primary BN wurtzite nanostructures description has the ability to maintain the natural characteristics of the nanostructure, concerning the bulk of the crystal. Some the studied physical properties are in a great agreement with results of experiments, such as energy gap, bond angles and bond lengths between multiple bonds, vibrational modes and some other properties. The numerous arrangements are able to be recognized by the proposed structure. BN-

based gas sensors nanostructures are up to date field that is unveiled in the current work using the existing wurtzoid structures. BN-based gas sensor nanostructures are seldom theoretically searched in previous studies, giving importance for the attempts in the current work.

Theory

The "B3LYP (Becke, three-parameter, Lee-Yang-Parr) with valence triple-zeta basis 6-311G** via all-electron density functional theory (DFT)" was used. The above basis in the first asterisk shows that a polarization d-functions set was added to heavy atoms. The later asterisk refers to that the polarization p-functions set was added to atoms of hydrogen. These bases are also occasionally showing 6-311G (d, p) [7]. The frequencies are multiplied by an appropriate scaling factor (0.967) usually assigned to the present method with the basis set (B3LYP/6-311G**) [8].

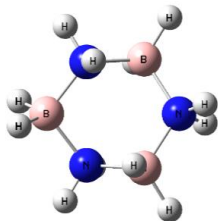
Wurtzoids has been proposed as a wurtzite molecular structure to simulate nanoparticles. These molecules demand to identify two indicators (a and c), as in the common structure (hexagonal) unlike diamondoids (cubic). Such molecules are a BN- (0.3) nanotube bundle. This structure is applied to the bare and H-passivated formations without opposite perceivable structural reform. Bare wurtzoids are investigated, B_3N_3 , B_7N_7 , $B_{13}N_{13}$, $B_{21}N_{21}$, and $B_{39}N_{39}$. As for $B_3N_3H_{12}$, $B_7N_7H_{14}$, $B_{13}N_{13}H_{26}$, $B_{21}N_{21}H_{30}$, and $B_{39}N_{39}H_{54}$ are in passivated clusters after complete hydrogen passivation at their surface.

These molecules of H-passivated are BN cyclohexane ($B_3N_3H_{12}$), wurtzoid ($B_7N_7H_{14}$), wurtzoid2c ($B_{13}N_{13}H_{26}$), triwurtzoid ($B_{21}N_{21}H_{30}$), and triwurtzoid2c ($B_{39}N_{39}H_{54}$) [7,8], figure (1) shows these H-passivated molecules. Removing H atoms from these figures gives bare wurtzoids. A molecule with double (c) constant in wurtzite structure called wurtzoid 2c by adding the suffix, -2c, in fact, three BN (3,0) nanotubes are combined to produce this molecule called triwurtzoid by adding the prefix, tri-. Triwurtzoid 2c indicate the wurtzite structure has a double c constant and bundled of three BN (3.0) nanotubes together. The BN cyclohexane (Bare B_3N_3 and whole passivated H $B_3N_3H_{12}$); this molecule of hexagonal ring-form are both wurtzoids and diamondoids building block[20][21][22]

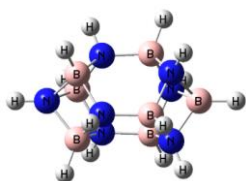
The package "Gaussian 09" interface was used to apply the current molecular optimization and calculations molecular vibrational modes

[11] and taking benefit of a 'GausView05' program.

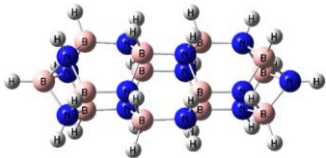
BN cyclohexane



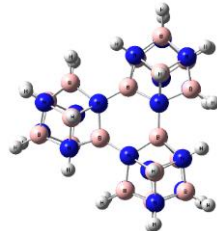
BN wurtziod



BN wurtzoid2c



BN triwurtziod



BN triwurtziod 2c

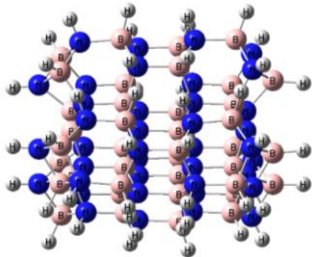


Figure 2: BN molecules and wurtzoids of H-passivated which consist of Silver, blue, white balls refer to B, N, H atoms, respectively.

Results and Discussion

BN bare triwurtzoid 2c ($B_{39}N_{39}$) and passivated triwurtzoid 2c ($B_{39}N_{39}H_{54}$) densities of states are indicated in Figures (3a) and (3b), respectively, the energy levels functions after geometric optimization and the densities of states decrease with the wurtzoid's size, this means the wurtzoid's structures with H-passivated near to nanoscales led to decreased values of these gaps. Splitting of states is another explanation for this increase of energy gaps of additional states [12]. Moreover, the density of states has degenerated where the states are high due to the high symmetry.

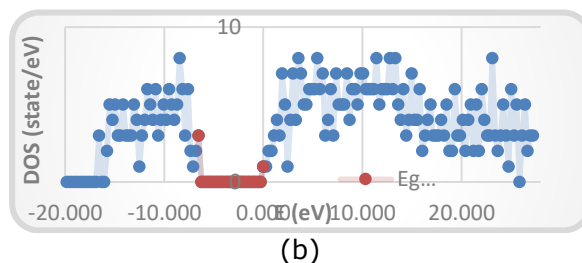
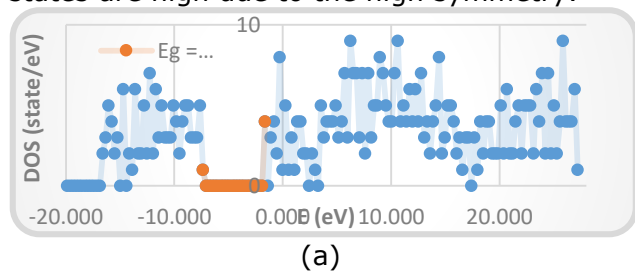


Figure 3: Density of states for (a) $B_{39}N_{39}$ and (b) ($B_{39}N_{39}H_{54}$)

On the other hand, the energy gaps decrease with the existence of hydrogen passivation on the surface of the BN molecules, as shown in figure (4), and denotes that the energy gaps of bare and H-passivated BN molecules functions to form the total number of atoms B and N, as well as "Low Unoccupied Molecular Orbitals" LUMO and "High Occupied Molecular Orbitals" HOMO, which express the unoccupied and occupied levels of BN molecules of bare and passivated as a function of the same atom. The energy gaps at nanoscale decrease due to quantisation confinement. Therefore, energy gap values are calculated theoretically with H-passivated high BN molecules. The experimental values of BN Wurtzite [13], when compared with the gap values in existing H-atoms on their surface, each molecule represents with the stoichiometry, BNH_6 , $B_3N_3H_{12}$, $B_7N_7H_{14}$, $B_{13}N_{13}H_{26}$, $B_{21}N_{21}H_{30}$, and $B_{39}N_{39}H_{54}$, giving 8.03, 8.12, 7.90, 7.45, 7.21, and 6.54 eV respectively, while bare BN clusters, BN, B_3N_3 , B_7N_7 , $B_{13}N_{13}$, $B_{21}N_{21}$ and $B_{39}N_{39}$ illustrate that the theoretical results (1.96, 5.35, 4.71, 3.42, 5.68, and 5.58 eV) are very close to the experimental value of BN wurtzite of energy gaps, the experimental value of BN wurtzite, which can be seen under the dashed line in Figure (4).

The bare clusters of BN have values less than H-passivated of these clusters, due to their dangling bonds inserts levels of energy into the forbidden gap. On the other hand, the levels of LUMO are more sensitive than the HOMO levels for surface effects, though there is the appearance of a small difference between the two levels in both cases (Bare and Passivated), especially when the clusters are large [9] as seen in two curves. The LUMO levels have a large difference between both due to the added electron [14]. The values of energy gaps result in this work for bare clusters of BN approximated to the experimental bulk value. Thus, it can be considered a good result [15].

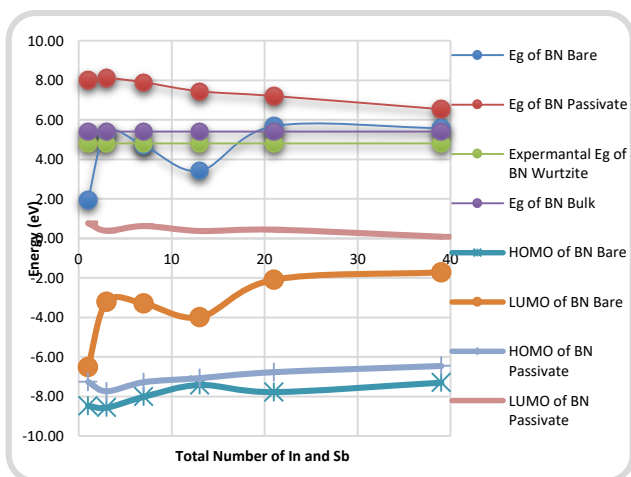


Figure 4: Energy gaps in the experimental value of bulk BN, E.g. of BN, LUMO and HOMO levels (Bare and Passivate), B as a function of the total number of B and N atoms in BN Wurtizet.

The bond lengths distribution is shown in figure (5) for the BN wurtzoid bare and H-passivated. The results gave existence of three kinds of bonds, i.e., N-H bonds are the first bonds, followed by B-H bonds, and the most significant bond lengths distribution is in B-N bonds. These bonds values are almost compatible with the shown experimental values [16], which may be due to the current determinations similar to the surface identifications, leading to the deviation of several bonds from perfect length values due to the reconstruction. The result concluded that the length of the bond is always given less value than 0.3Å of the experimental value.

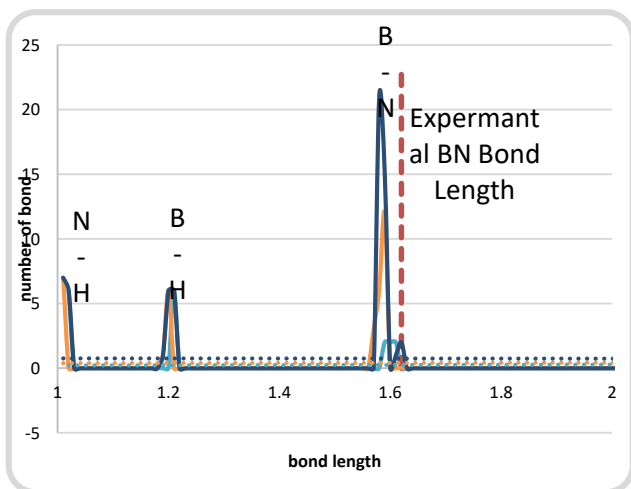


Figure 5: Distribution of Bonds density in BN Wurtizet (Bare and Passivated), the experimental value is indicated by the dashed line of BN bond length at 1.68 Å.

The tetrahedral angle density distribution of the BN (bare and passivated) is shown in Figure (6). The bulk part far from the surface has a value of 109.5° for all tetrahedral angles [17]. The B13N13H26 tetrahedral angle gives the nearest value to the quixotic value of 109.5° compared to the other. The explanation is the surface influence reconstruction, which affects every atom in passivated BN because each atom has a bond with the hydrogen atoms on the surface, but bare BN atoms affects by some atoms [18].

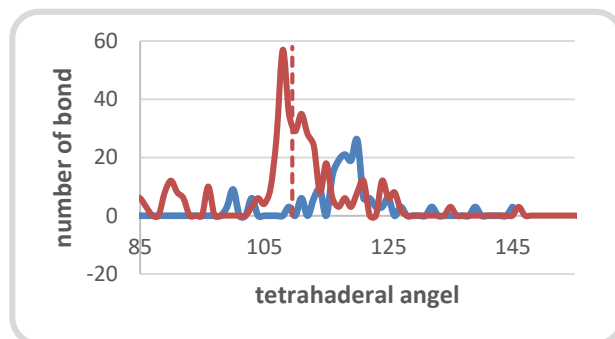
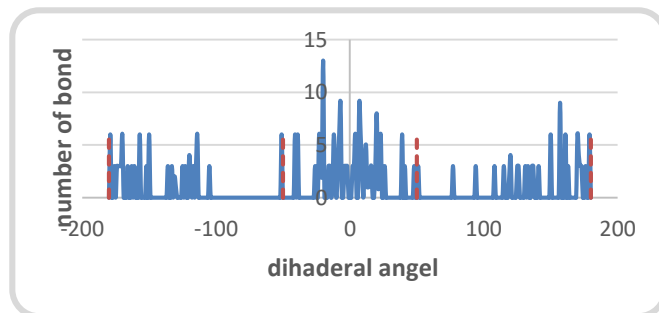
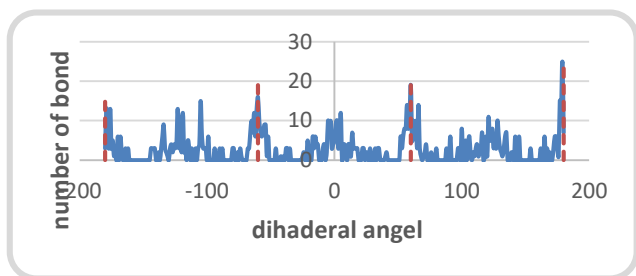


Figure 6: "Distribution tetrahedral angle densities in BN Wurtizet (bare and passivated). The bulk structure at 109.5° value is indicated by the dashed line.

According to the same approach, a comparison was made between the dihedral angle densities of the B₃₉N₃₉ and B₃₉N₃₉H₅₄, where each angle of the dihedral must have one of the angles -180°, -60°, 60°, or 180° values in the bulk wurtzite structure [19]. These results are a good agreement for -180° and 180° in B₃₉N₃₉H₅₄, as given in figure (7b). While, it is sufficiently exact for the -60° and 60° values for B₃₉N₃₉ shown in figure (7a), the -60° and 60° were not found to become close to ideal values



(a)



(b)
Figure 7: Densities of dihedral angle in (a) B₃₉N₃₉ (b) B₃₉N₃₉H₅₄. The bulk wurtzite

structure is indicated by the dashed line, i.e., ±60° or ±180°.

Figure (8) shows the force constants of BN passivated located as functions of vibration frequency aloof from the statistical variation between them in vibration frequency numbers. These figures are nearly like in shape. Trends can be split into the two parts, in all figures. The first part start at almost 0 cm⁻¹ and ends about 700 cm⁻¹. However, the second part begins at 760 cm⁻¹ and ends at about 3500 cm⁻¹.

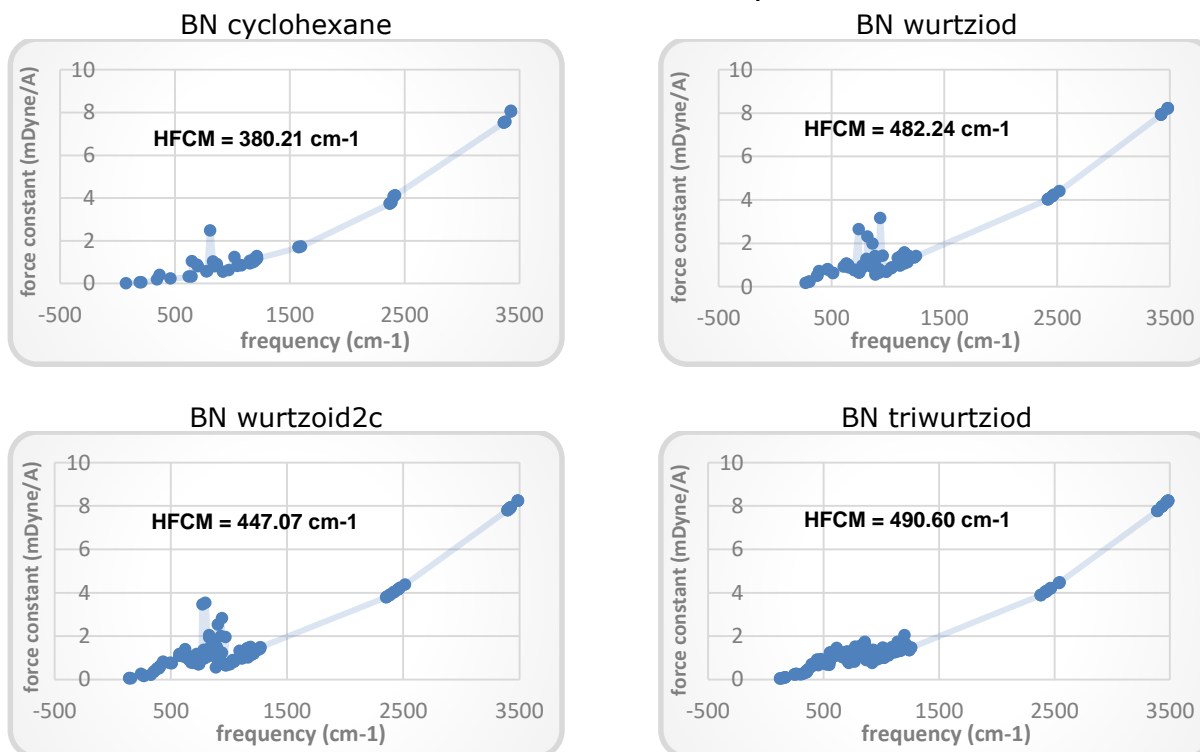


Figure 8: Force constant as a vibration frequency function in multi passivated BN.

Figure (9) elucidates the little vibrations masses of BN passivated also have two similar parts according to force constant. Furthermore, they exhibit reduced masses at >1 in the first part and approaching 1 in the second. The second part exhibits H vibrations, whereas, the first part demonstrates BN

vibrations with reduced masses >1. The related equation between the frequency and the "force constant and reduced mass of vibration" is:

$$\nu = \frac{1}{2\pi} \sqrt{\frac{k}{\mu}} \text{-----(1)}$$

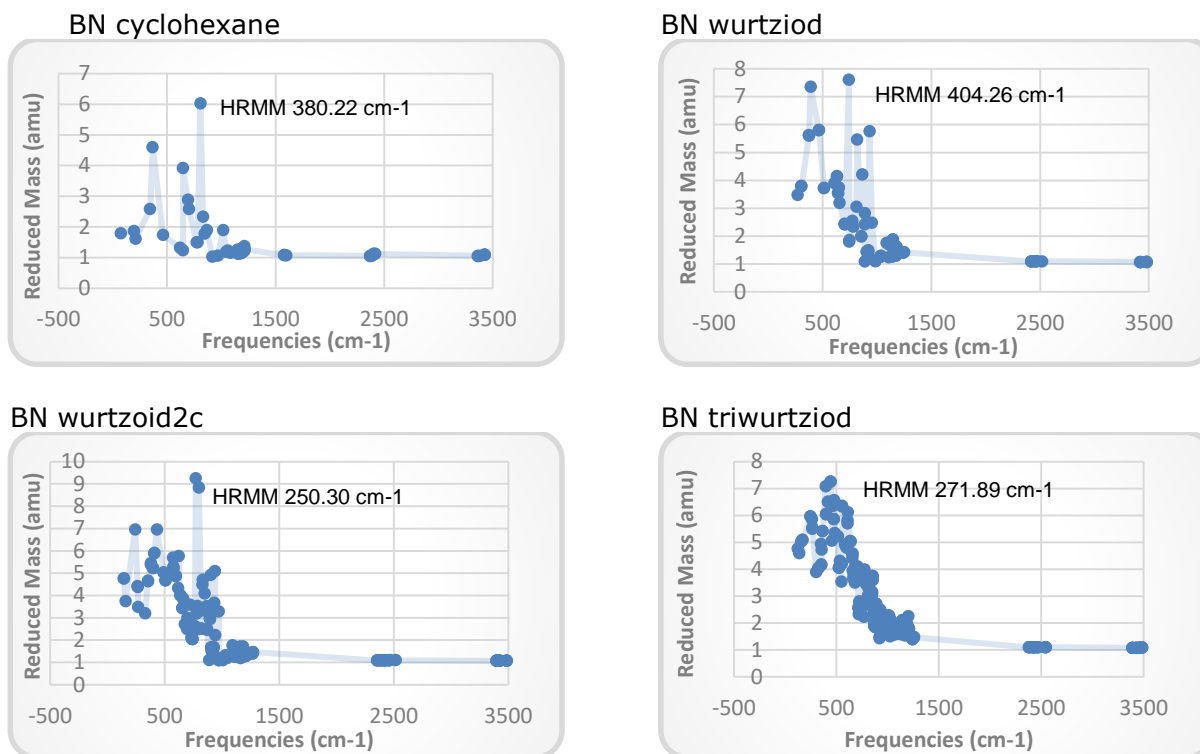
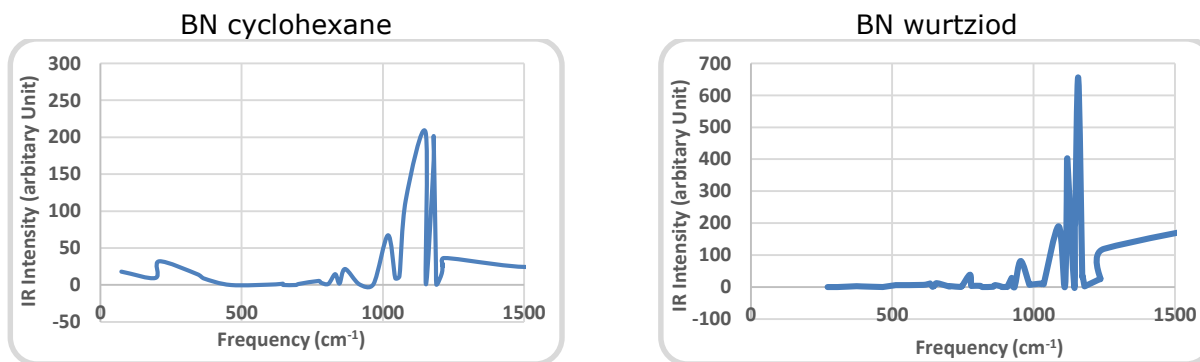


Figure 9: Reduced mass as a vibration frequency function in multi passivated BN.

The intensity of infrared radiation as a function of frequency as shown in Figure (10). A comparison of infrared values with the size of boron nitride indicates that there is a directly proportional increase indicating that the hydrogen as a sensor gave the ability to increase the vibrations of boron nitride when the size increased. It is also found that the sensitivity area values starts when it is greater than 1100 m⁻¹ and up to about 1180 m⁻¹.

Figure (11) shows the relationship between Raman spectra. It is found that the frequency increased and it's evident that the value of the frequency increases with the increase in size compared to different values for Raman spectra, and this makes hydrogen, as a sensor supports the increase in frequency, which confirms the increase of crystalline bond with the increasing size compared to the vibration characteristics.



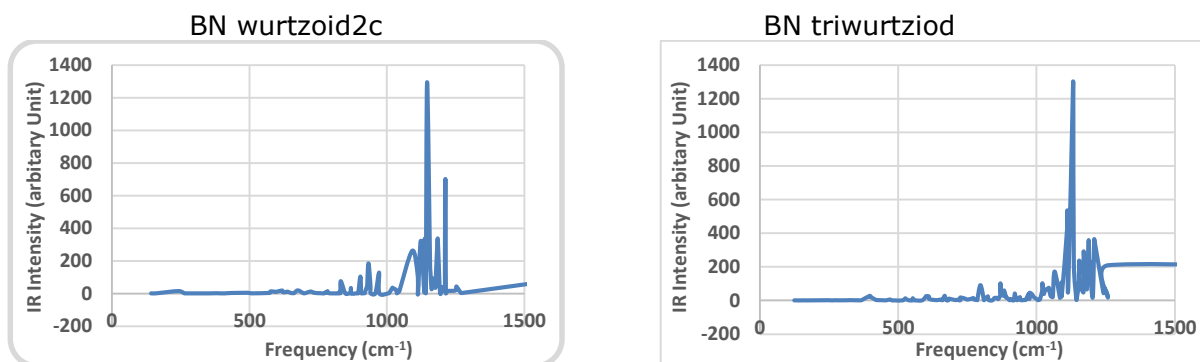


Figure 10: IR Intensity as a vibration frequency function in multi passivated BN.

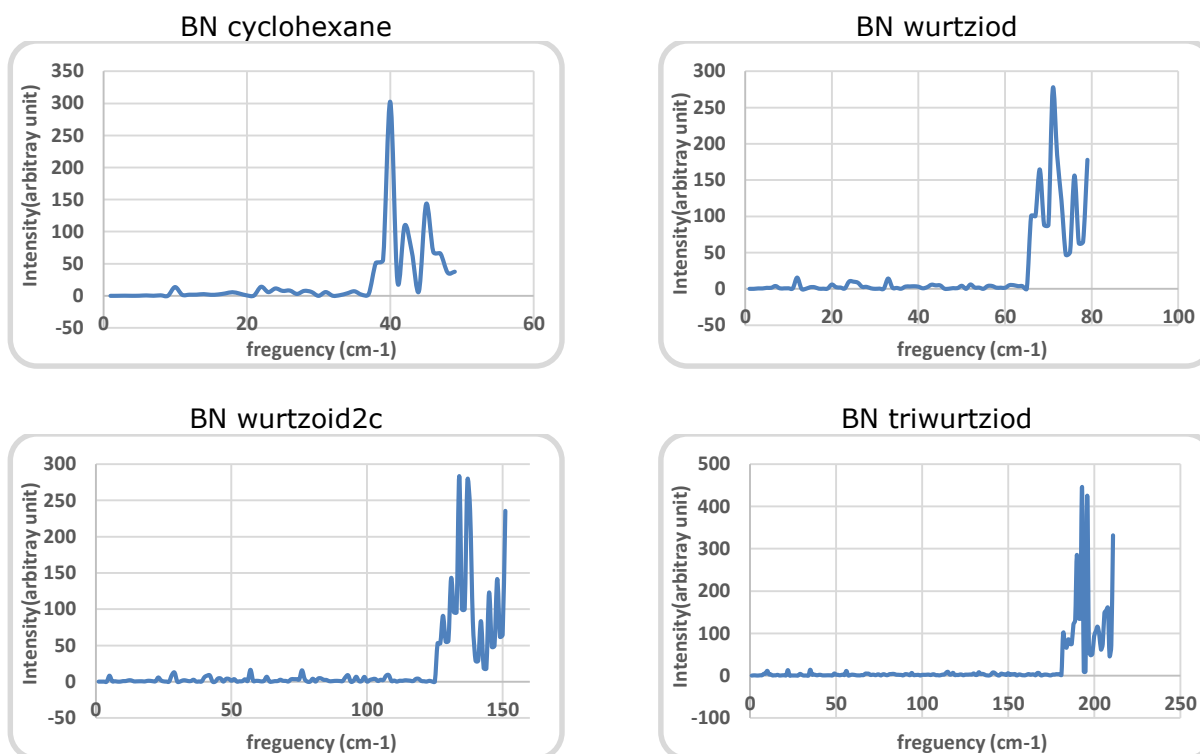


Figure 11: Raman Intensity as a vibration frequency function in multi passivated BN.

Conclusions

The structural properties of boron nitride BN approach values of both nanoparticles and bulk. The values obtained for the bond length where the highest peaks approach to the ideal and practical with the same percentage of error mentioned by many sources. For the vibrational properties, we found that the longitudinal infrared radiation was influenced by the presence of hydrogen, where the intensity is increasing intensively with the increase in size. In contrast, we found that Raman spectra horizontally increased (degeneracy) in frequency with size increasing. HFCM and HRMM were found to have different values at $B_{21}N_{21}H_{30}$ and $B_7N_7H_{14}$, respectively. Boron nitride BN nanotubes are

suitable as a hydrogen additive sensor as proven in previous experimental results. The results show that the boron has little correlation with the hydrogen. In contrast, the correlation was the highest value between N and H, which made the compound responsible for the sensing ability.

References:

- [1] Haynes, William M., ed. [CRC Handbook of Chemistry and Physics](#) (92nd ed.). Boca Raton, FL: [CRC Press](#). p. 5.6. [ISBN 1439855110](#); (2011).
- [2] Kawaguchi, M.; et al. "Electronic Structure and Intercalation Chemistry of Graphite-Like Layered Material with a Composition of BC_6N ". *Journal of Physics and Chemistry of Solids*. [doi:10.1016/j.jpcs.2007.10.076](#); (2008).

- [3] Griggs, Jessica. "[Diamond no longer nature's hardest material](#)". New Scientist. Retrieved; (2014).
- [4] Osamah Ibrahim Khalaf, Bayan Mahdi Sabbar "An overview on wireless sensor networks and finding optimal location of node", Periodicals of Engineering and Natural Sciences, Vol 7, No 3 (2019)
- [5] Zedlitz, R.; "Properties of Amorphous Boron Nitride Thin Films". Journal of Non-Crystalline Solids. 198–200 (Part 1): 403. [Bibcode: 1996JNCS. 198. 403Z](#). [doi:10.1016/0022-3093\(95\)00748-2](#); (1996).
- [6] Bilal k.Al-Rawi; Asmiet Ramizy; "Modeling the Vibrational Properties of InSb Diamondoids and Nanocrystals Using Density Functional Theory; Journal of Inorganic and Organometallic Polymers and Materials; doi.org/10.1007/s10904-018-1037-y; (2018).
- [7] M. A. Abdulsattar, Mohammed T, Hussein, and H. A. Hammeed " Ab initio structural and vibrational properties of GaAs diamondoids and nanocrystals" AIP Advances 4,127119(2014).
- [8] NIST Computational chemistry comparison and benchmark database, release 15b, 2011. <http://cccbdb.nist.gov/> (Accessed November 1, 2015).
- [9] M. A. Abdulsattar "Molecular approach to hexagonal and cubic diamond nanocrystals" Carbon Letters Vol. 16, No. 3, 192-197 (2015).
- [10] M. A. Abdulsattar, "Capped ZnO (3, 0) nanotubes as building blocks of bare and H passivated wurtzite ZnO nanocrystals", Superlattices Microstruct. 85, 813 (2015).
- [11] Gaussian 09, Revision A.02, M. J. Frisch, G. W. Trucks, H. B. Schlegel et al., Gaussian, Inc., Wallingford CT, (2009).
- [12] Mohammed T.Hussain, H.A.Fayyadh; " Theoretical Modeling of the Electronic Properties Core and Surface of CdSe_{1-x}Te_x Chalcogenide Nanocrystals Via DFT Calculation " Chalcogenide letters, vol.13 no. (12),2016 p.537-545; (2016).
- [13] S. Bhusal, J.A. Rodriguez Lopez, J. Ulises Reveles, Tunna Baruah, and Rajendra R. Zope, "Electronic and Structural Study of Zn_xS_x [x = 12, 16, 24, 28, 36, 48, 96, and 108] Cage Structures" J. Phys. Chem. A 2017, 121, 3486–3493, DOI: 10.1021/acs.jpca.6b12172; (2017).
- [14] M. A. Abdulsattar, "GaN wurtzite nanocrystals approached using wurtzoids structures and their use as a hydrogen sensor: A DFT study" Superlattices and Microstructures 93 163e170; (2016).
- [15] Osamah Ibrahim Khalaf, Ghaidaa Muttasher et al., "Improving video Transmission Over Heterogeneous Network by Using ARQ and FEC Error Correction Algorithm", vol. 30, no.8, pp.24-27, Nov 2015
- [16] C. Stampfl and C. G. Van de Walle, "Density-functional calculations for III-V nitrides using the local-density approximation and the generalized gradient approximation", Phys. Rev. B 59, 5521 (1999).
- [17] Hamsa Naji Nasir, Mudar A. Abdulsattar, and Hayder M. Abduljalil, Adv. in Cond. Matt. Phys., Vol. 2012, Article ID 348254, 5 pages, (2012).
- [18] Volker Jonas, Gernot Frenking, "Studies on the boron–nitrogen bond length of the classical donor–acceptor complex H₃N–BF₃", Journal of the Chemical Society, Chemical Communications, Issue 12, DOI: 10.1039/C39940001489, (1994)
- [19] Osamah Ibrahim Khalaf, Ghaida Muttashar Abdulsahib and Muayed Sadik, 2018. A Modified Algorithm for Improving Lifetime WSN. Journal of Engineering and Applied Sciences, 13: 9277-9282